Effective Date: 10/11/2024
Expiration Date: 10/11/2029

XRISM/ Resolve
CMO
10/11/2024
RELEASED

INSTRUMENT CALIBRATION REPORT

RESOLVE MODULATED X-RAY SOURCE (MXS) PULSE PARAMETERS

RESOLVE-SCI-RPT-0054

REVISION (C)

XRISM-RESOLVE-CALDB-MXSPARAM-218

X-ray Imaging and Spectroscopy Mission (XRISM) Project

NASA/GSFC Code 461

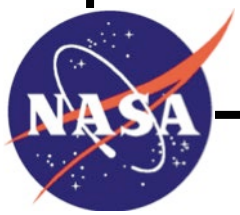

National Aeronautics and
Space Administration

Goddard Space Flight Center
Greenbelt, Maryland

Check https://ipdtdms.gsfc.nasa.gov
to verify that this is the correct version prior to use

RESOLVE MODULATED X-RAY SOURCE (MXS) PULSE PARAMETERS

Signature/Approval Page

Prepared by: Renata Cumbee, Makoto Sawada, Cor de Vries, and the Resolve Instrument Team

Reviewers/Approvers:

Megan Eckart
Marcellus Ajiboye
Renata Cumbee
Caroline Kilbourne
Maurice Leutenegger
Michael Lowenstein
Scott Porter
Tahir Yaqoob

Approved by:

Megan Eckart

***** Electronic signatures are available on-line at: https://ipdtdms.gsfc.nasa.gov*****

Preface

This document is an XRISM Project signature-controlled document. Changes to this document require prior approval of the applicable Product Design Lead (PDL) or designee. Proposed changes shall be submitted in the Technical Data Management System (TDMS) via a Signature Control Request (SCoRe) along with supportive material justifying the proposed change. Changes to this document will be made by complete revision.

All of the requirements in this document assume the use of the word "shall" unless otherwise stated.

Questions or comments concerning this document should be addressed to:
XRISM Configuration Management Office
Mail Stop: 461
Goddard Space Flight Center
Greenbelt, Maryland 20771

Change History Log

Revision	Effective Date	Description of Changes (Reference the SCoRe Approval Date)
-	01/10/2020	Released per RESOLVE-SCoRe-0264
A	10/30/2023	Released per RESOLVE-SCoRe-0563
B	09/16/2024	Changed title page to "XRISM-RESOLVE-CALDB-MXSPARAM-218," updating " MXSPARAMS" to "MXSPARAM" to match CalDB. No other changes. Released per RESOLVE-SCoRe-0571
C	10/11/2024	Update Ref. 8 information now that Sawada, et al., Proc. SPIE, 2024 has been published. (Previously it was noted as in prep.) Release per RESOLVE-SCoRe-0575

NOTE to editors: The document name will be XRISM-CAL-RPT-XXXX, where XXXX is assigned by the TDMS system. The document will be cross-referenced in TDMS to the filename in the format XRISM-XXX-CALDB-FILEDESC-NN where XXX is the instrument or component (e.g., RESOLVE), FILEDESC refers to a specific calibration report (e.g., rmfparams) and NN the corresponding number assigned to that report by the SDC. For example the calibration report addressing the Resolve LSF calibration may be assigned XRISM-RESOLVE-CALDB-RMFPARAMS-01, that addressing the Resolve gain calibration XRISM-RESOLVE-GAINPIX-CALDB-02, etc. (where the numbers are to be provided by the SDC).

These documents are updated as needed, e.g. when the relevant CalDB files, or the relevant calibration data analysis, is revised. The document version will be assigned by the TDMS system. The tracking tool should be used to record changes.

This document must include the CalDB file name, an explanation of how the data were collected and the analysis conducted and, if using standard Ftools, the software version number. All revisions are consolidated into the same document to maintain a full record of all changes.

Table of Contents

1 Introduction

1.1 Purpose

This document describes the CalDB file that contains calibration data for the pulse properties of the x-ray spectra produced by the direct and indirect MXS sources.

The modulated x-ray source (MXS) will be used for on-orbit calibration and for monitoring the time-dependent gain of Resolve. The MXS uses light-sensitive photocathodes illuminated by two LEDs to generate an electron beam, which impacts a target anode, generating x-rays. The electron beam, and thus x-rays, will only be generated while the LED is emitting light, allowing short duration pulses. By operating the MXS with a short pulse period and filtering events based on the MXS status, it is possible to continuously monitor the performance of each pixel during astronomical observations while avoiding contamination of the astrophysical data from the MXS photons.

Two types of MXS sources exist: a direct source, which illuminates the Resolve detector array with the x-ray spectrum generated by the Cr/Cu anode, producing Cu Kα and Kβ, Cr Kα and Kβ, and bremsstrahlung; and an indirect fluorescent source which illuminates the Resolve detector array with an x-ray spectrum generated by an Al/Mg fluorescence target, producing Al Kα and Kβ and Mg Kα and Kβ lines, shown in Table 1. The two types of MXSs are present as a redundant pair, such that MXS1 and MXS2 are the nominal direct and indirect sources, and MXS2 and MXS3 are the redundant direct and indirect sources. The flux of the fluorescent sources is significantly weaker than that of the direct sources, and will be pulsed at much higher duty cycles (~50%) when used. The MXS is described in further detail in [1] and [2], and the Resolve MXS calibration plan is described in [3].

	Kα	Kβ
Target	E (keV)	E (keV)
Cr	5.4147	5.9547
Cu	8.0778	8.9053
Mg	1.2536	1.3022
Al	1.4867	1.5574

Table 1: MXS Target center of mass energies for the direct (Cr and Cu) and indirect (Mg and Al) MXS (from [6]).

1.2 Scientific Impact

For observations that take place while the MXS is operating in pulse mode, the MXS CalDB file is used to remove MXS calibration photons from the astrophysical data set via good-time-interval (GTI) cuts. In addition, the inverse of the clean celestial source data GTI are used to

select the MXS-on calibration emission-line data (described in Table 1) in order to construct a gain history file. The pulse profile of the x-rays from MXS has two components: the main pulse and an afterglow. The LED turn-on times with small offsets (delays) are used to define starts of the MXS illumination intervals, while the shape of the pulse afterglow tail, in combination with various thresholds, is used to define the stop of the intervals. The CalDB file provides tables to calculate the main pulse start and stop offsets and afterglow durations as functions of the LED operation parameters. The two ftools `rslmxstime` and `rslmxsgti` are used to calculate the MXS GTI. `Rslmxstime` reads the MXS CalDB file and assigns LED on time intervals for each LED. `Rslmxsgti`, internally runs `rslmxstime` and uses its outputs to calculate time intervals with and without MXS illumination for specified combinations of LEDs.

2 First Delivery 20190215

CalDB Filename	Validity date	File(s) as Delivered	Delivery Date	Comments
xa_rsl_mxsparam_20140101v001.fits	20150101 00:00 UT	Original ASCII files: xa_rsl_mxsparam_20140101v001_trial005_t1_offset.txt xa_rsl_mxsparam_20140101v001_trial005_t1_0.0001.txt xa_rsl_mxsparam_20140101v001_trial005_t1_0.0003.txt xa_rsl_mxsparam_20140101v001_trial005_t1_0.001.txt xa_rsl_mxsparam_20140101v001_trial005_t1_0.003.txt xa_rsl_mxsparam_20140101v001_trial005_t1_0.005.txt	20190215	Extension # 1 2 3 4 5 6

2.1 Data Description

The experiments described in this section are described in detail in [3]. In brief, timing calibration tests were performed at SRON using the engineering model (EM) MXS (the former ASTRO-H engineering model), in which the relevant capacitor has been replaced by the intended capacitance for the XRISM Resolve flight model. Measurements were made of the x-ray pulses as a function of LED current and for different pulse lengths. The MXS main pulse start times have offsets due to the digital-to-analog converter (DAC) inside the filter wheel electronics (FWE) and depend on the LED current, while the shape of the MXS afterglow tail depends on the duration of the main pulse. Additional measurements made with the flight model (FM) MXS will be included in future versions of the MXS CalDB file and this document.

2.2 Data Analysis

The main pulse start and stop offsets measurement

Timing measurements were performed to describe the MXS pulse start time and stop time offsets for three LED currents: 1.0 mA, 2.0 mA, and 4.0 mA. It was found that the stop time offset was small and only significant at the lowest current (~10 µsec at 1.0 mA). On the other hand, the start time offset was significant, ranging from ~0.1-0.3 ms. The dependence of the pulse start offset on the LED current, shown in Figure 1, was well reproduced by the form:

$$Offset(Current) = Current^{P0} \times 10^{P1} \quad , \qquad (1)$$

where *Offset* and *Current* are given in units of ms and mA, respectively, and the parameters were derived to be **P0** = –0.58113571 and **P1** = –0.59194637. This pulse start offset is defined as the time at which the pulse reaches the half-maximum intensity. The above model reproduces the measured offsets with an accuracy of a few µsec.

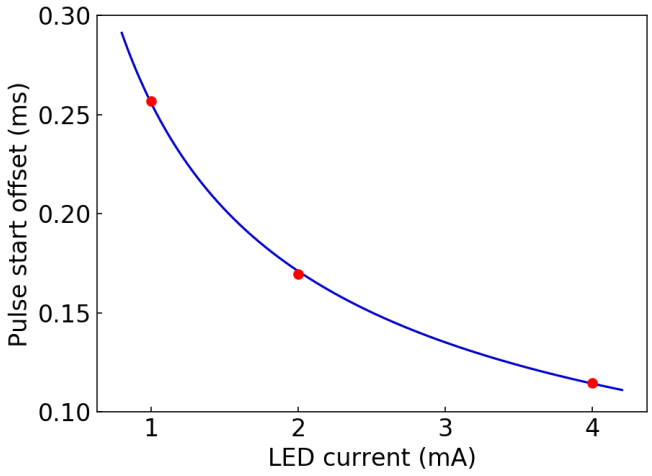

Figure 1: Pulse start offsets for various LED currents.

The afterglow measurement

Pulse tail afterglow measurements were performed for two different parameter sets: a 1.0 ms pulse length with a pulse period of 109.375 ms and a 3.125 ms pulse length with a 31.25 ms pulse period. For the 1 ms pulse length case, the afterglow profile is fitted in times between 10 and 110 ms after the main pulse start. The profile is well reproduced by a two-component exponential decay function with e-folding times of $\boldsymbol{\tau_1}$ = 5.4 ms and $\boldsymbol{\tau_2}$ = 76 ms, whose normalizations to the main pulse are $\boldsymbol{a_1}$ = 1.51E-03 and $\boldsymbol{a_2}$ = 4.39E-05, respectively. For the times closer to the main pulse (< 10 ms), shorter e-folding times are found, as shown in Figure 6 of [3], and more modelling is necessary to describe the afterglow shape accurately.

From the comparison of the afterglows for the two different pulse lengths (1 and 3 ms), it is found that the afterglow of the 3 ms pulse length can be reproduced as a sum of shifted and added afterglow tails of three 1 ms length pulses mimicking a 3 ms pulse. By generalizing this relation, we get the following form of the afterglow for a pulse length of *PulseLength* ms:

$$Afterglow(t; PulseLength) = \sum_{i=1,2} a_i * \exp(-t/\tau_i) * (1 - \exp\left(\frac{PulseLength}{\tau_i}\right))/(1 - \exp\left(\frac{1}{\tau_i}\right)) \quad (2)$$

where *t* is the time after the main pulse start (without an offset), *Afterglow* is relative intensity of the afterglow normalized to the average intensity of the main pulse, and $\boldsymbol{\tau_{1,2}}$ and $\boldsymbol{a_{1,2}}$ are the e-folding times and normalizations $\boldsymbol{\tau_1}$, respectively, given above. The afterglow shape is shown in Figure *2*.

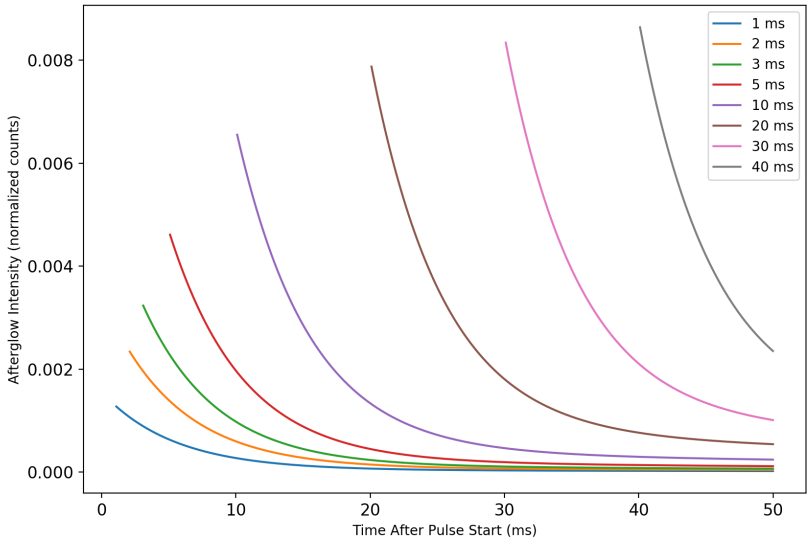

Figure 2: Pulse afterglow shapes for various pulse lengths. The pulse intensities are normalized to the same flux level.

2.3 Results

The first extension, `MXSOFFSET` describes the offsets of the main pulse start and stop times as functions of the LED current. This extension has nine columns: `ILED` for the LED current, `LED#STARTDELT` (# = 1-4: the LED IDs, where the LED IDs are consistent with the MXS IDs) for the start offsets, and `LED#STOPDELT` (# = 1-4) for the stop offsets, and 400 rows with currents ranging from 0.01 to 4 mA. The ftool `rslmxstime` reads the filter wheel electronics (FWE) extension of the Resolve HK file to get LED currents used in an observation. Offset times

are obtained by interpolating the LED#STARTDELT and LED#STOPDELT columns for each LED at the LED current used in the observation. Note that the delay due to the time offset between FWE and spacecraft is not included in this table; the software automatically reads this from the MXSSCDLT keyword of the MXSOFFSET header. This spacecraft time offset is applied to and shifts the entire pulse including the afterglow.

Each of the second and later extensions (MXSAFTERGLOWnnn: nnn = 001, 002, …) describe the afterglow duration vs commanded pulse length assuming a specific discrete value of threshold on the decaying pulse amplitude (threshold fraction, stored in the AGTHRESH keyword) that defines the end of the afterglow. The extension has five columns, PLSLEN for the pulse length and LED#AGDELT (# = 1-4) for the afterglow durations, and 501 rows with pulse lengths ranging from 0 to 50 ms. The data tables are first interpolated at the threshold value specified by a user (decaythresh). Then, the afterglow duration is obtained for each LED by interpolating this table at the pulse length recorded in the FWE extension of the Resolve HK.

Extension 1: MXSOFFSET

The start time offsets, LED#STARTDELT (# = 1-4), are populated as a function of the LED current (ILED) using the model shown in Figure 3, which is obtained by extrapolating the Equation 1 to lower currents down to 0.01 mA. The stop time offsets, LED#STOPDELT (# = 1-4), are currently all assumed to be zero because the measured stop time offsets are small, and the illumination stop times are typically determined rather by the afterglow tail. Currently, identical start and stop offset tables are assumed for all LEDs. This can be modified during later stages of calibration.

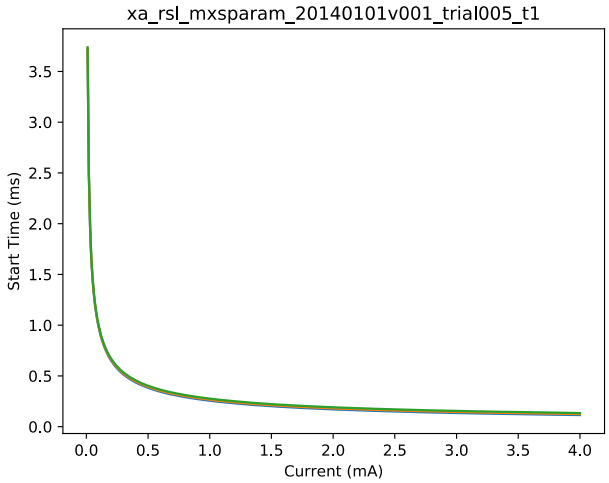

Figure 3: Pulse start offset model.

Extension 2+: MXSAFTERGLOW

The pulse afterglow duration, `LED#AGDELT` (# = 1-4) is shown in Figure 4 (as a function of pulse length (PLSLEN) for 0-50 ms) for threshold fractions (`decaythresh`) of 0.0001, 0.0003, 0.001, 0.003, and 0.005, using the model described by Equation (3). Here, the time origin of the afterglow duration is the end of the pulse, such that `LED#AGDELT` (# = 1-4) is added to the commanded pulse stop. The lowest threshold of 0.0001 is taken from the recommended value in [5]. The higher thresholds are added in case users want to have a smaller dead time for science events at the expense of increased background. When the threshold fraction is smaller than ~0.001, the afterglow pulse intensity never reaches the threshold fraction for larger pulse lengths (>10 ms for the threshold fraction 0.0001). In this case, the afterglow duration AGDELT is set to the last value at which the threshold fraction was reached, and the curve becomes flat, as shown in Figure 4 for the threshold fractions of 0.0001 and 0.0003. With larger threshold fractions, the modeled afterglow intensities are always below the threshold for small pulse lengths. In such cases, the duration is set to 0. Currently, an identical afterglow duration is assumed for all MXSs. This can be modified during later stages of calibration and as needed.

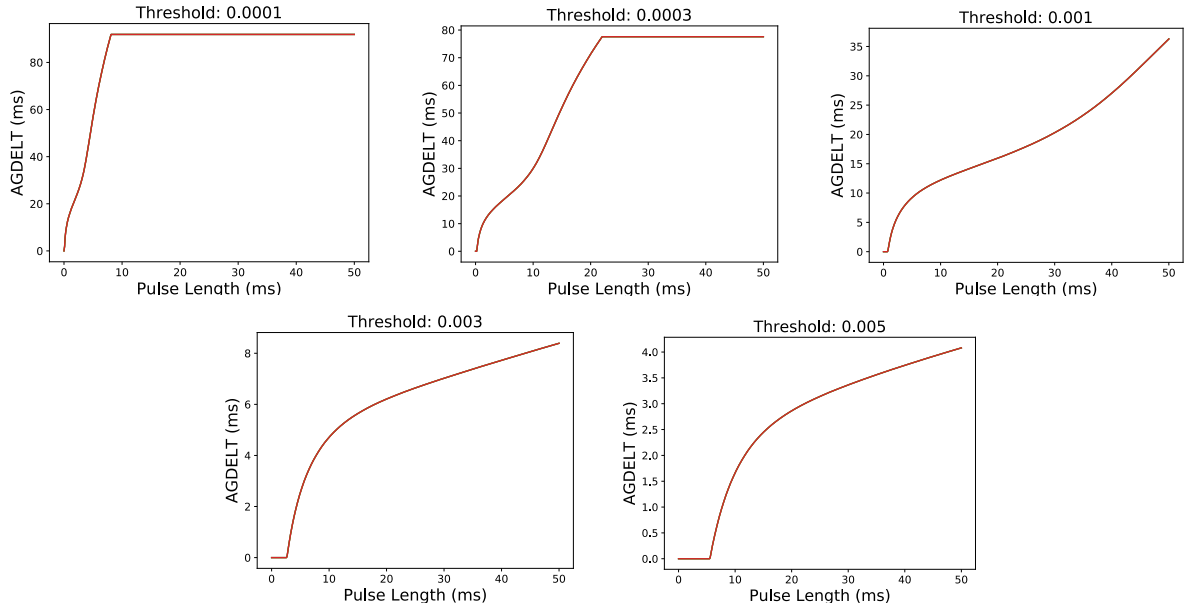

Figure 4: The afterglow duration (LED#AGDELT) as a function of pulse length (PLSLEN) for thresholds of 0.0001, 0.0003, 0.001, 0.003, and 0.005.

2.4 Remarks

The related ftools, `rslmxstime` and `rslmxsgti`, use the MXS CalDB file described in this document (specified by the `mxsledfile` parameter) by default, in combination with the FWE extension of the Resolve HK file and the `decaythresh` parameter (see Section 2.1). These

tools also have options to override the CalDB file. When a numerical value is specified for the `mxsoffset` parameter, the value is used to shift the main pulse start, instead of using `LED#STARTDELT`. Similarly, when a numerical value is specified for the `dtafterglow` parameter, it overrides the afterglow duration derived by `LED#AGDELT` and `decaythresh`. The stop offsets and the afterglow durations are degenerate since both quantities are measured from the commanded LED off-time. If both quantities are non-zero, only the larger of the two is applied to the end of the pulse for the stop time of the GTI. These parameters are applied uniformly to all LEDs. For more details, see the help files for `rslmxstime` and `rslmxsgti`.

As noted in Section 2.2, the measured pulse start offset is defined as the time at which the pulse reaches the half-maximum intensity. This is because the primary purpose of the time offset measurement was to define reference point to calibrate the Resolve absolute timing using the MXS. By choosing this MXS start time offset, `rslmxsgti` does not eliminate the very beginning of the MXS LED illumination from the astrophysical events, which could contaminate science data. This can be avoided by setting the mxsoffset parameter to 0. An alternative approach is to introduce a gap in the start time offset between the two types of GTIs: one for extracting astrophysical data and the other for the MXS photons used for gain tracking (see Section 1.2). This way, we can use a shorter offset to define the stop times of the former GTI and can reduce the contamination from the MXS photons to science data while enabling the start times of the latter GTI to be unchanged or optimized independently. There is a plan for adding such an additional parameter to this CalDB file, and when that plan is finalized, the document will be updated accordingly (see Section 3.3 and Figure 10 for additional discussion). It is currently assumed that all four MXSs (two driven by the primary and two by the redundant FWE power supplies) have identical properties on the main pulse start/stop offsets and afterglow shape. Possible differences among units can be incorporated in this CalDB file based on ground measurements of the flight model during the Resolve calibration campaign.

3 Revision 20230308 (with addition 20230707)

CalDB Filename	Validity date	File(s) as Delivered	Delivery Date	Comments
xa_rsl_mxsparam_20190101v002.fits	20190101 00:00 UT	Original ASCII files:		Extension #
		xa_rsl_mxsparam_20190101v002_TEST_MXSOFFSET.txt	2023-03-08	1
		xa_rsl_mxsparam_20190101v002_TEST_MXSAFTERGLOW001.txt		2
		xa_rsl_mxsparam_20190101v002_TEST_MXSAFTERGLOW002.txt		3
		xa_rsl_mxsparam_20190101v002_TEST_MXSAFTERGLOW003.txt		4
		xa_rsl_mxsparam_20190101v002_TEST_MXSAFTERGLOW004.txt		5
		xa_rsl_mxsparam_20190101v002_TEST_MXSAFTERGLOW005.txt		6
		xa_rsl_mxsparam_20190101v002_TEST_description.txt		N/A
		mxscaldb_inputparams_v2.csv	2023-07-07	The parameters delivered here supersede those in the description file for the 20230308 delivery.

3.1 Data Description

The analysis in this delivery is based on [7] and to be reported in detail elsewhere [8]. The experimental data are from spacecraft-level measurements performed at TKSC using the FM MXS and FM FWE along with the XRISM Resolve flight instrument. Measurements were performed for the MXS1 and MXS3 units. Aging tests were performed during the thermal vacuum test at TKSC on the nominal MXS1, in which the MXS was operated in the high count rate regime to reduce the photocathode efficiency and accelerate aging before launch. We assume that the afterglow profiles for MXS2 and MXS4 are similar to those of MXS3, which was not aged.

3.2 Data Analysis

The main pulse start and stop offsets measurement

Measurements were performed to calibrate the MXS pulse start time and stop time offsets for LED currents ranging from 0.93 to 4.9 mA for MXS1 and MXS3. The start offset is due to the design of the FWE driver circuit, whose length depends on the LED current.

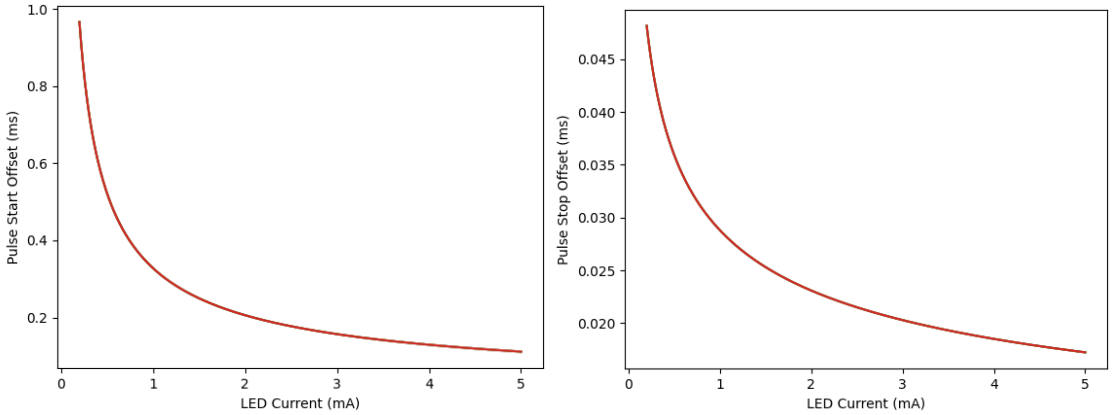

Figure 5: Pulse start (left) and stop (right) offsets for all LED currents.

The pulse start and stop offsets are described by Eq. (1)**,** with the derived parameters **P0** and **P1** shown in Table 2. The pulse rise/fall time has a small dependence on the LED current, which is shown in Figure *7* as the difference in the pulse falling edge between the highest and lowest LED current. Thus, to determine the absolute timing offset, multiple MXS illumination data sets with different LED current settings are needed. The data sets used include both the LED1 and LED3 cases as the pulse rise/fall times were found to be common to both units. The pulse start and stop offsets are shown in Figure 5.

Table 2: Parameters for pulse rise and fall delay.

	RISEP0	RISEP1	FALLP0	FALLP1
LED1	-0.671523	-0.484173	-0.319239	-1.540378
LED2	-0.671523	-0.484173	-0.319239	-1.540378
LED3	-0.671523	-0.484173	-0.319239	-1.540378
LED4	-0.671523	-0.484173	-0.319239	-1.540378

The afterglow measurement

The afterglow tail profile was characterized using the component-level test data taken in 2019 using the FM LED1 and FWE, but ground support electronics as described in [7], and with further analysis performed in thermal vacuum test in 2022. Pulse tail afterglow measurements

were performed for a variety of parameters for LED1 (aged) and LED3. As in the first delivery, the afterglow profile is represented by a multi-component exponential decay function, but with two differences. As described in [7], the afterglow profile has a small dependence on the LED current because it is dependent on the effective pulse length, which is reduced by the pulse start offset

$$\mathbf{t_{len,eff}} = \mathbf{t_{len}} - \boldsymbol{start\_Offset} + \boldsymbol{stop\_Offset} \quad (3)$$

where $\mathbf{t_{len}}$ is the commanded pulse length, and ***start_Offset*** and ***stop_Offset*** describe the pulse start and stop offsets (Eq. 1).

To derive the tail amplitudes and decay timescales, $\boldsymbol{a_{0,i}}$ and $\boldsymbol{\tau_i}$, the MXS profile was fitted with the following multiple-component exponential decay function including the LED current dependence on the pulse start offset,

$$\boldsymbol{Afterglow}(t, t_{len}, t_{offset}) = \sum_i \boldsymbol{a_{0,i}} \left[\boldsymbol{exp}\left(\frac{t_{len}}{\tau_i}\right) - \boldsymbol{exp}\left(\frac{t_{Offset}}{\tau_i}\right)\right] * \boldsymbol{exp}\left(\frac{t}{\tau_i}\right) \quad (4)$$

where $\mathbf{t_{len}}$ is the commanded pulse length, $\boldsymbol{t_{offset}}$ is the pulse start offset, $\boldsymbol{a_{0,i}}$ and $\boldsymbol{\tau_i}$ are the amplitude and decay timescale for the ith level component (`AMPi` and `TAUi`). For τ_i >>t_{len}, t_{offset} >> stop_Offset,

$$\boldsymbol{Afterglow}(t, t_{len,eff}) \approx \sum_i \boldsymbol{a_{0,i}} * \frac{t_{len,eff}}{\tau_i} * \boldsymbol{exp}\left(-\frac{t}{\tau_i}\right) \quad (5).$$

To derive the tail amplitudes and decay timescales, $\boldsymbol{a_{0,i}}$ and $\boldsymbol{\tau_i}$, the afterglow profile for LED1 and LED3 were fitted with the multiple-component exponential decay function, Eq. (4). A four-component model was found to be sufficient to reproduce the data. The measured parameters are given in Table 3. There is no afterglow profile measurement for the indirect MXS sources, therefore, we use the parameters of the LED3 which was not aged for the LED2 and LED4. The afterglow shape is shown in Figure 6 for a range of effective pulse lengths. The shortest component ($\boldsymbol{\tau_1}$~0.1ms) can be ignored as it originates from the capacitor in the driver circuit. It is not likely to scale with the relation assumed in equations (4) and (5), and the component is only significant very close to the main pulse (<0.5ms).

Table 3: Measured pulse profile parameters used to characterize the afterglow decay.

	AMP1	AMP2	AMP3	AMP4	TAU1	TAU2	TAU3	TAU4
LED1	0.024346	0.012189	0.003899	0.007523	0.132624	4.949066	28.228596	2565.067259
LED2	0.036352	0.033002	0.001972	0.004547	0.107417	4.446187	92.19754	996.645121
LED3	0.036352	0.033002	0.001972	0.004547	0.107417	4.446187	92.19754	996.645121
LED4	0.036352	0.033002	0.001972	0.004547	0.107417	4.446187	92.19754	996.645121

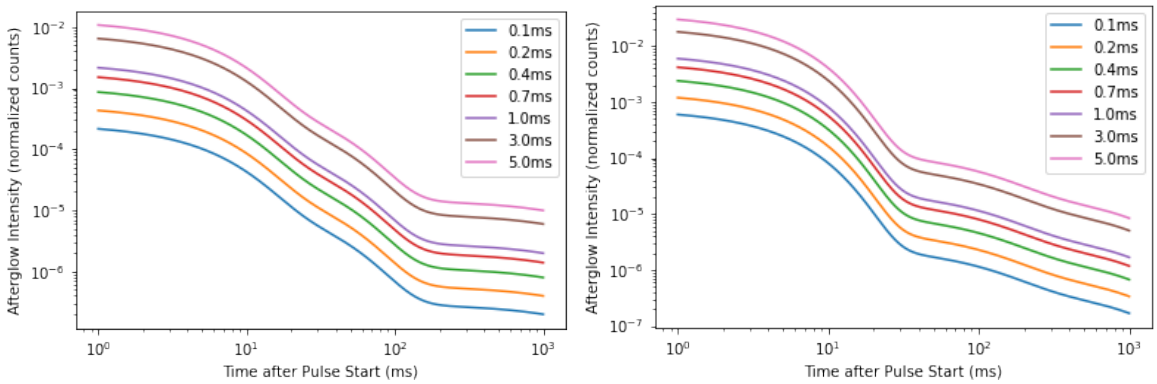

Figure 6: Pulse afterglow shapes for LED1 (left) and LED3 (right) for various effective pulse lengths. LED1 was aged, so the afterglow profile parameters for LED3 are assumed for LED2 and LED4.

3.3 Results

The data in the first extension, `MXSOFFSET` describes the offsets of the main pulse start and stop times as functions of the LED current. Here, we update each column for `LED#STARTDELT` and `LED#STOPDELT` based on measurements taken during the TC7 thermal-vacuum testing campaign. Note that the delay due to the time offset between FWE and spacecraft is not included in this table; the software automatically reads this from the `MXSSCDLT` keyword of the `MXSOFFSET` header. In addition to `MXSSCDLT`, there is an additional delay internal to FWE, `SCDLTNOM` of 4 μs for the nominal MXS units, and `SCDLTRED` of 4 μs for the redundant MXS units. These spacecraft time offsets are applied to and shift the MXS GTI start/stop.

As described in Section 2.4, the measured pulse start and stop offset is defined as the time at which the pulse reaches the half-maximum intensity. This is because the primary purpose of the time offset measurement was to define reference point to calibrate the Resolve absolute timing using the MXS. By choosing this MXS start and stop time offset, `rslmxsgti` does not eliminate the very beginning of the MXS LED illumination from the astrophysical events, and a small fraction of events spills over outside the MXS start and stop, which could contaminate science data. A constant 0.04 ms margin for the start and stop offsets (as shown in Figure *7*) is sufficient to eliminate the additional MXS counts without negatively impacting the science data for a broad range of LED currents. A new keyword, `MXSMARGN`, is introduced to exclude these additional counts at the very beginning and end of the MXS pulse. `MXSMARGN` is subtracted from LED pulse-command-on and the PulseStartoffset to determine START of GTI, and added to the effective pulse length and pulse stop offset to determine the STOP of the GTI when `LED#AGDELT` is not used to define the stop of the GTI.

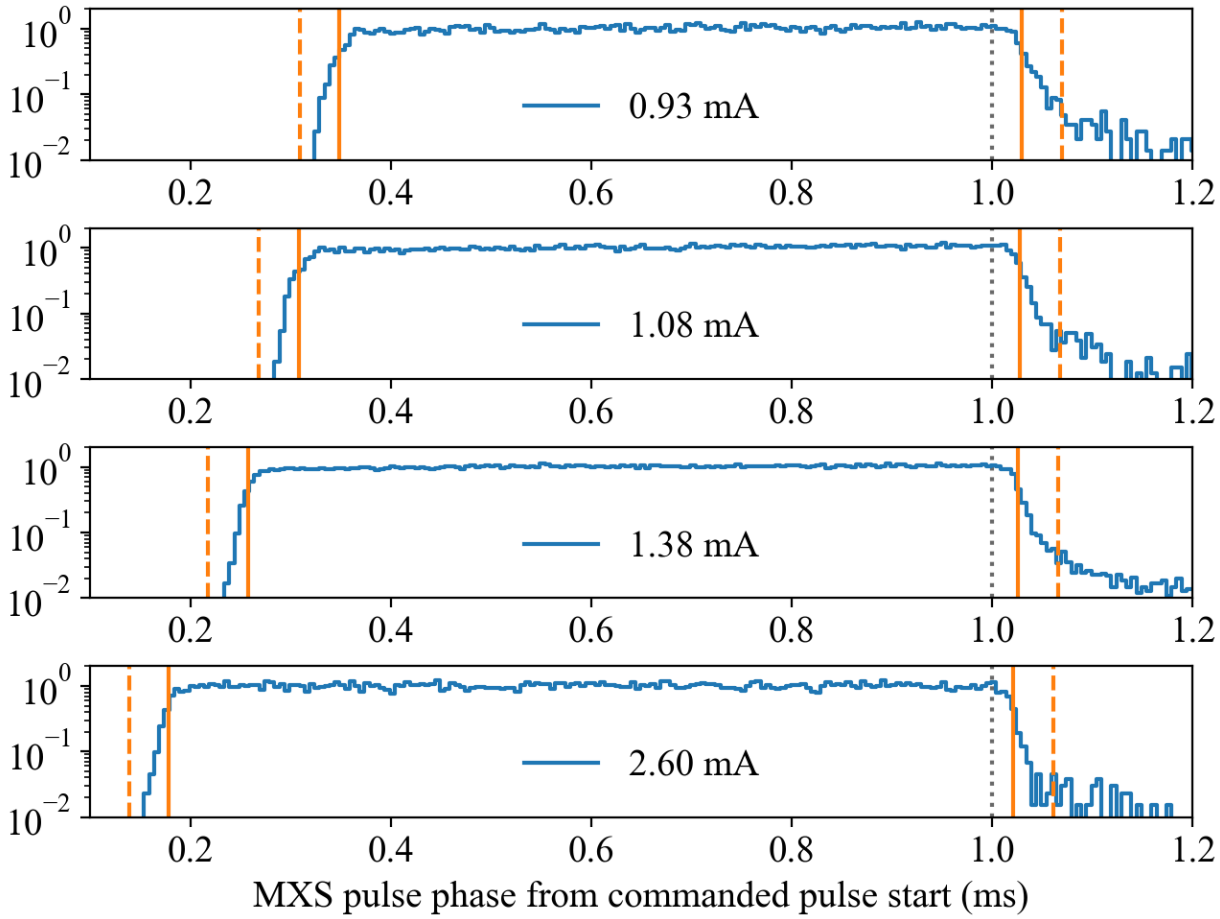

Figure 7: Example MXS pulse profiles for LED3. The orange bars on the left and right are the pulse rising and falling edges, respectively, while the grey dotted line represents the commanded pulse stop. A 0.04ms MXSMARGN is shown with the dashed line to the left of the start time, and the right of the stop times.

Each of the second and later extensions (`MXSAFTERGLOWnnn`: nnn = 001, 002, …) describe the afterglow duration vs effective pulse length assuming a specific discrete value of threshold on the decaying pulse amplitude (threshold fraction, stored in the `AGTHRESH` keyword) that defines the end of the afterglow. Here, we update the pulse afterglow duration, `LED#AGDELT` (# = 1-4) based on the analysis of the thermal vacuum (TC7) measurements using the model described by Equation (5). In this release, the pulse afterglow is considered as a function of effective pulse length (`EFFPLSLEN`, see Eq.(3)) instead of the commanded pulse length (`PLSLEN`) to ensure that the dependence the afterglow profile has on the LED current is included.

The extension has five columns; `EFFPLSLEN` for the effective pulse length and `LED#AGDELT` (# = 1-4) for the afterglow durations, and 501 rows with pulse lengths ranging from 0 to 50 ms. The data tables are first interpolated at the threshold value specified by a user (`decaythresh`). Then, the afterglow duration is obtained for each LED by interpolating this table at the pulse length recorded in the FWE extension of the Resolve HK.

Extension 1: MXSOFFSET

The start time offsets, `LED#STARTDELT` (# = 1-4) and stop time offsets, `LED#STOPDELT` (# = 1-4), are populated as a function of the LED current (`ILED`) using the model shown in Figure 5, which is obtained by extrapolating Equation 1 to lower currents down to 0.01 mA. Currently, identical start and stop offset tables are assumed for all LEDs. This assumption can be modified during later stages of calibration. In this release, the start and stop offsets are updated, and the LED current range is increased from 4mA to 5 mA to cover the maximum values used in ground measurements.

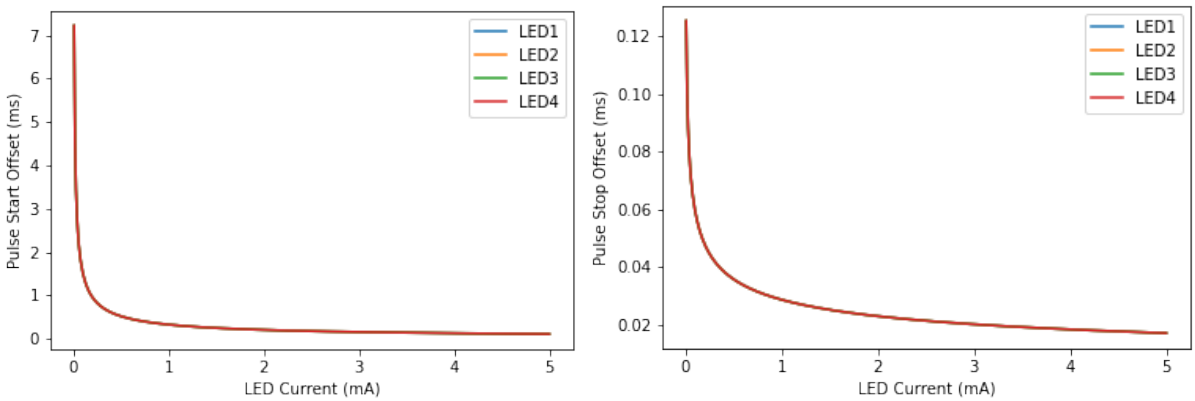

Figure 8: Pulse Start offset model (left) and pulse stop offset model (right).

Extension 2+: MXSAFTERGLOW

The pulse afterglow durations, `LED#AGDELT` (# = 1-4) are populated as a function of effective pulse length (`EFFPLSLEN`), using the model described by Equation (5). The time origin of the pulse afterglow in this release is defined at the start of the pulse, such that `LED#AGDELT` (# = 1-4) is added to the pulse commanded start.

The afterglow durations are shown in Figure 9 for threshold fractions (`decaythresh`) of 0.0001, 0.0003, 0.001, 0.003, and 0.005 for LED1 and LED3. As aging tests were performed on MXS1, in which the photocathode efficiency was reduced on purpose, we assume that the afterglow durations for MXS2 and MXS4 are similar to those of MXS3 which was not aged.

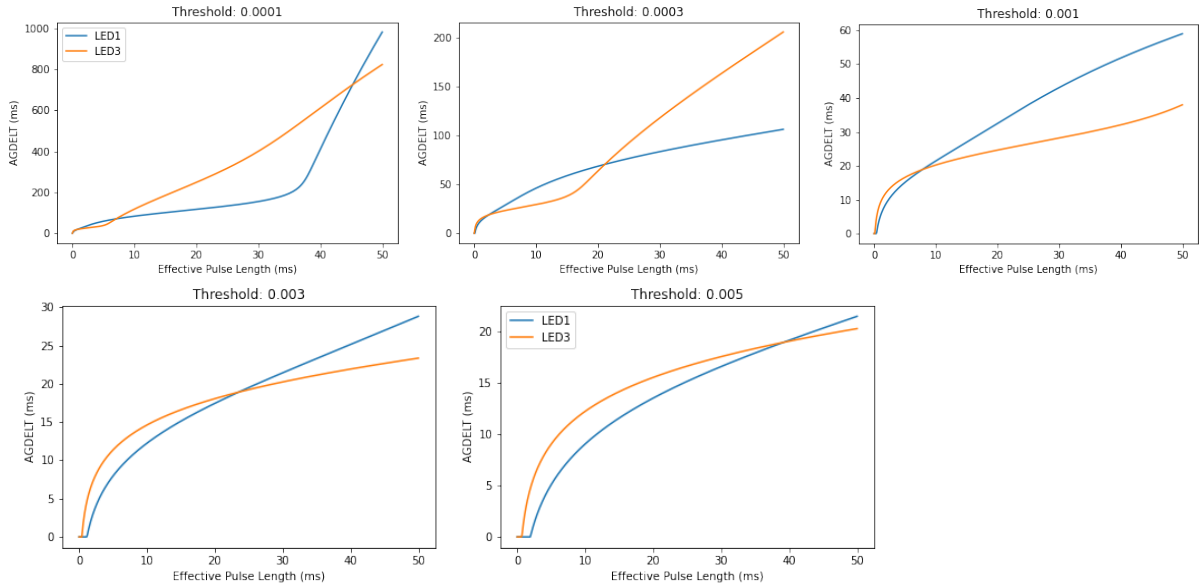

Figure 9: The afterglow duration (LED#AGDELT) as a function of effective pulse length (EFFPLSLEN) for thresholds of 0.0001, 0.0003, 0.001, 0.003, and 0.005.

MXSCOEFFS

In addition to the interpolated data used to determine the start and stop offsets (`MXSOFFSET`) and the afterglow durations (`MXSAFTERGLOW`), the parameters used to calculate these MXS properties are provided. The rise and fall parameters `RISEP0, RISEP1, FALLP0, FALLP1,` and afterglow parameters `AMP#` and `TAU#` (1-4) are populated as lists with length 4 (for `LED#`=1-4) for each parameter. This allows `LED#STARTDELT` and `LED#STOPDELT` to be derived from the pulse command on and off and LED current. The LEDiAGDELT can then be derived from the effective pulse length (Equations (4) and (5)) to include the dependence on LED current. This allows a thorough elimination of the MXS counts from the very beginning and the very end of the MXS illumination, and effectively eliminates the contamination from astrophysical events. The amplitude `AMP1` for the shortest component (`TAU1`~0.1ms) is set to zero as it can be ignored as described in Section 3.2.

3.4 Comparison with previous release

The analysis in this delivery is based on the thermal vacuum test in 2022, which included spacecraft-level measurements using the FM MXS, FWE, and Resolve flight instrument. This is an improvement over the measurements using the EM MXS in the initial release. Additionally, prior to the thermal vac test campaign in 2022, aging tests were performed on MXS1, which affected the afterglow profile. The thermal vacuum testing campaign included measurements for a variety of MXS parameters (ILED, pulse spacing, etc) for MXS3 in addition to MXS1. As MXS1 was aged, the parameters defined for MXS3 are used for MXS2 and MXS4 as they are

expected to be more similar. In this delivery, the exponential decay function that describes the afterglow profile depends on the effective pulse length, as compared to the commanded pulse length, which was used in the initial delivery. This dependence on the effective pulse length incorporates the effect of the ILED on the afterglow profile.

Based on the analysis of the data in this release, in the first extension, MXSOFFSET, the start and stop offsets are updated, and the stop offsets no longer have a value of zero. In addition, the LED current range is increased from 4 mA to 5 mA to cover the maximum values considered in in this analysis.

For extensions 2-6, the MXSAFTERGLOW, three major changes are included compared to the initial release. The afterglow durations are populated as a function of effective pulse length (EFFPLSLEN) instead of commanded pulse length (PLSLEN) using the function described by Equation (5) to ensure that the dependence the afterglow profile has on the LED current is included, and the time origin of the pulse afterglow is defined at the commanded pulse start instead of the commanded pulse stop, making this CalDB file incompatible with previous versions of the software.

3 new parameters were introduced in this release. In addition to the delay due to the time offset between FWE and spacecraft (MXSSCDLT), an additional 4 μs delay internal to FWE was included, SCDLTNOM for the nominal MXS units, and SCDLTRED for the redundant MXS units. An additional time offset is used to ensure that any MXS counts are excluded from astrophysical events. Analysis shows that a constant 0.04 ms margin for the start and stop offsets (as shown in Figure 7) is sufficient to eliminate additional MXS counts without negatively impacting the science data for a broad range of LED currents. A new keyword, MXSMARGN, is introduced to exclude these additional counts at the very beginning and end of the MXS pulse.

This delivery additionally includes the MXS offset and afterglow parameters, with values shown in Table 2 and Table 3, to allow software using this CalDB file the option of calculating the MXS parameters from the functions (i.e. equations (1) and (4)) in addition to the tabulated MXS offsets and afterglow durations in Extension 1-6.

4 Revision 20230728

CalDB Filename	Validity date	File(s) as Delivered	Delivery Date	Comments
xa_rsl_mxsparam_20190101v003.fits	20190101 00:00 UT	Original ASCII files		Extension #
		xa_rsl_mxsparam_20190101v003_TEST_MXSOFFSET.txt	2023-07-28	1
		xa_rsl_mxsparam_20190101v003_TEST_MXSAFTERGLOW001.txt		2
		xa_rsl_mxsparam_20190101v003_TEST_MXSAFTERGLOW002.txt		3
		xa_rsl_mxsparam_20190101v003_TEST_MXSAFTERGLOW003.txt		4
		xa_rsl_mxsparam_20190101v003_TEST_MXSAFTERGLOW004.txt		5
		xa_rsl_mxsparam_20190101v003_TEST_MXSAFTERGLOW005.txt		6
		mxscaldb_inputparams_v003a.csv	2023-07-28	7

4.1 Data Description

The test data used to derive the parameters in this delivery are the same as those in the previous delivery. Additional analysis was performed following the analysis in the Resolve timing coefficients report [9] In the analysis method, the absolute timing offset is derived simultaneously with the MXS pulse offsets, so these always need to be updated in a pair. In the second delivery (20230308), the MXS timing offset analysis was with the relative timing coefficients a = b = c = 0 (for a description of these coefficients, refer to [9]), while the analysis in this delivery was performed with the relative timing calibration applied (see xa_rsl_coeftime_20190101v002.fits /build 6).

4.2 Data Analysis

The main pulse start and stop offsets measurement

From the first (20190215) and second (20230308) deliveries, the pulse start and stop offsets are known to be described by Eq. (1). In the Resolve ground tests, measured pulse start and stop timings are commonly affected by the PSP's absolute timing offset (Figure 10). Thus, to determine the MXS' start/stop offset and the PSP's absolute timing offset simultaneously, multiple MXS illumination data sets with different LED current settings are needed. The data sets used include both the LED1 and LED3 cases as the pulse start/stop offsets were found to be common to both units. The derived parameters **P0** and **P1** are shown in Table 4.

The pulse start and stop offsets are shown in Figure 11.

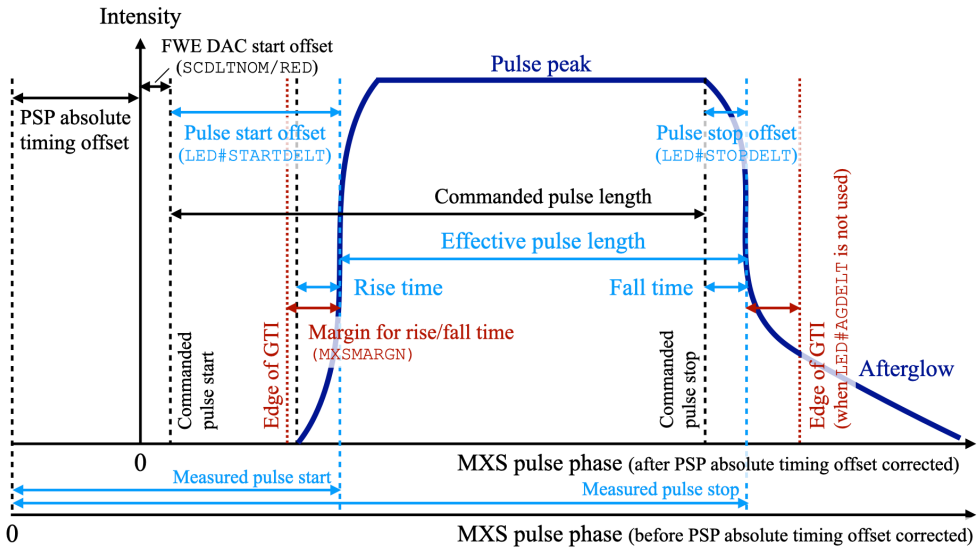

Figure 10: Timing diagram of MXS pulse start and stop measurements. The timings and time intervals that depend on the LED current are shown in light blue.

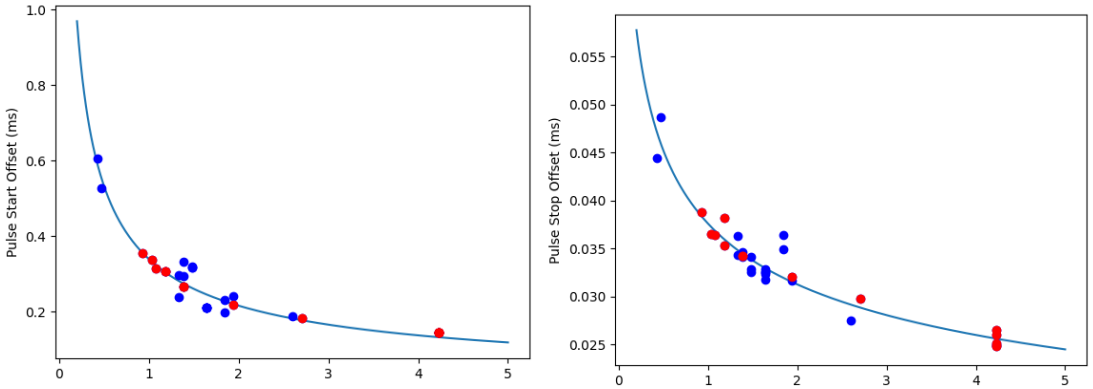

Figure 11: Pulse start (left) and stop (right) offsets for all LED currents. Start and stop offsets measurements for LED1 and LED3 are plotted for various LED current parameters. The red data points indicate a pulse spacing of 0.468ms, while the blue data points include pulse spacings ranging from 0.078 ms to 1.56ms.

Small deviations of measured pulse start from the model (described by **P0** and **P1**) show a correlation with the pulse spacing. Since this dependence is small over a wide range of pulse spacing and the origin is not known, we address this by increasing the `MXSMARGN` offset. Note that increasing `MXSMARGN` does not result in a significant loss of science data.

Table 4: Parameters for pulse rise and fall delay.

	RISEP0	RISEP1	FALLP0	FALLP1
LED1	-0.651124	-0.468494	-0.266760	-1.424992
LED2	-0.651124	-0.468494	-0.266760	-1.424992
LED3	-0.651124	-0.468494	-0.266760	-1.424992
LED4	-0.651124	-0.468494	-0.266760	-1.424992

4.3 Results

The data in the first extension, MXSOFFSET describes the offsets of the main pulse start and stop times as functions of the LED current. Here, we update each column for LED#STARTDELT and LED#STOPDELT based on updated analysis following the application of the Resolve timing coefficients [9]. Additionally, the maximum LED current is 10 mA in this extension to include all measurements performed during ground calibration.

In this delivery, the MXSMARGN offset is increased from 40 μs to 60 μs to enclose the deviations of the start offset caused by the pulse spacing

Extension 1: MXSOFFSET

The start time offsets, LED#STARTDELT (# = 1-4) and stop time offsets, LED#STOPDELT (# = 1-4), are populated as a function of the LED current (ILED) using the model shown in Figure 5, which is obtained by extrapolating the Equation 1 to lower currents down to 0.01 mA. Currently, identical start and stop offset tables are assumed for all LEDs. This can be modified during later stages of calibration. In this release, the start and stop offsets are updated, and the LED current range is increased from 5 mA to 10 mA to cover the maximum values used in ground measurements, especially for the indirect sources.

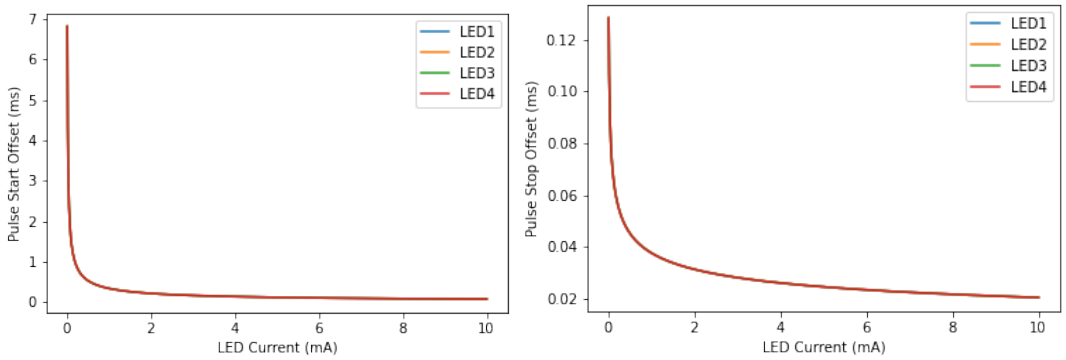

Figure 12: Pulse Start offset model (left) and pulse stop offset model (right)

Extension 2-6: MXSAFTERGLOW

No update from the second delivery.

Extension 7: MXSCOEFFS

In this delivery, the MXSCOEFFS extension is introduced to describe the MXS offset and afterglow duration parameters for each LED# (1-4). This extension includes one row with the rise and fall parameters RISEP0, RISEP1, FALLP0, FALLP1, and afterglow duration parameters AMP# and TAU# (1-4) populated as lists with length 4 (for LED# =1-4) for each parameter.

The afterglow parameters AMP# and TAU# (1-4) are described in the previous delivery in Table 3, while the rise and fall parameters RISEP0, RISEP1, FALLP0, FALLP1 are updated in this delivery, as described in Table 4.

This delivery is submitted with the afterglow parameters TAU1 and AMP1 are both set to zero to eliminate the contribution from the shortest component (TAU1~0.1ms), while in the previous delivery, only the AMP1 parameter was set to zero.

4.4 Comparison with previous releases

This CalDB file was derived using the same instrument-level test data as in the previous release, but with a different analysis approach. For this release the absolute timing offset [9] is derived simultaneously with the MXS pulse offsets and were updated as a pair (xa_rsl_coeftime_20190101v002.fits/build 6).

For Extension 1 (MXSOFFSET), the LED current range is increased from 5 mA to 10 mA, and the values for the start and stop offsets were updated based on the new analysis with the relative timing calibration applied.

Extension 7 was introduced to include the offset and afterglow parameters RISEP0, RISEP1, FALLP0, FALLP1, AMP# and TAU# (1-4) to allow direct calculations of the afterglow duration and offset in future CalDB builds. To reflect the updated analysis, these parameters were updated. The rise and fall parameters rise_p0, rise_p1, fall_p0, fall_p1 are updated based on Table 4, while afterglow parameters are almost unchanged from Table 3. The afterglow parameters TAU1 and AMP1 are both set to zero to eliminate the contribution from the shortest component (TAU1~0.1ms), while in the previous delivery, only the AMP1 parameter was set to zero.

Extensions 2-6 remained the same.

The MXSMARGN offset is increased from 40 μs to 60 μs from the previous delivery.

5 References

[1] Cor P. de Vries, et al., "Calibration sources and filters of the soft x-ray spectrometer instrument on the Hitomi spacecraft," JATIS, 4(1), 011204 (2017)
[2] M. E. Eckart, et al., "Ground calibration of the Astro-H (Hitomi) soft x-ray spectrometer," JATIS, 4(2), 021406 (2018)
[3] RESOLVE-SCI-PLAN-0034_Rev-_03-08-2019_Released.pdf, Ground Calibration Plan for the Resolve Instrument and Xtend Mirror Assembly
[4] SRON-XARM-RP-2018-006_mxs_timing.pdf
[5] RESOLVE-INST-RPT-0018-v1a, Proposed additional MXS requirements for XARM.
[6] M. Eckart, et al., "Natural Line Shapes of SXS Onboard Calibration Sources ASTH-SXS-CALDB-LINEFIT," 2016, https://heasarc.gsfc.nasa.gov/docs/hitomi/calib/hitomi_caldb_docs.html#SXS (19 October 2016).
[7] Makoto Sawada, et al., "Pulse parameters optimization of the modulated x-ray sources for the resolve microcalorimeter spectrometer on XRISM," Proc. SPIE 12181, Space Telescopes and Instrumentation 2022: Ultraviolet to Gamma Ray, 1218164 (31 August 2022); https://doi.org/10.1117/12.2630133
[8] Makoto Sawada, et al.,"Strategies for the in-orbit gain tracking using the modulated X-ray sources for the Resolve microcalorimeter spectrometer on XRISM," SPIE Proc. 13093 Space Telescopes and Instrumentation 2024: Ultraviolet to Gamma Ray, 1309364; https://doi.org/10.1117/12.3019586
[9] RESOLVE-SCI-RPT-0065_RevB_25-04-2023.pdf, Resolve Timing Coefficients